

Source-To-Sink Aeolian Fluxes From Arid Landscape Dynamics in the Lut Desert

Colin Chanteloube, Laurie Barrier, Reza Derakhshani, Cyril Gadal, Régis Braucher, Vincent Payet, Laëtitia Leanni, Clément Narteau

▶ **To cite this version:**

Colin Chanteloube, Laurie Barrier, Reza Derakhshani, Cyril Gadal, Régis Braucher, et al.. Source-To-Sink Aeolian Fluxes From Arid Landscape Dynamics in the Lut Desert. Geophysical Research Letters, 2022, 49, 10.1029/2021GL097342 . insu-03643047

HAL Id: insu-03643047

https://insu.hal.science/insu-03643047

Submitted on 18 Aug 2022

HAL is a multi-disciplinary open access archive for the deposit and dissemination of scientific research documents, whether they are published or not. The documents may come from teaching and research institutions in France or abroad, or from public or private research centers.

L'archive ouverte pluridisciplinaire **HAL**, est destinée au dépôt et à la diffusion de documents scientifiques de niveau recherche, publiés ou non, émanant des établissements d'enseignement et de recherche français ou étrangers, des laboratoires publics ou privés.

Copyright

Check for updates

AGU ADVANCING EARTH AND SPACE SCIENCE

Geophysical Research Letters®

RESEARCH LETTER
10.1029/2021GL097342

Key Points:

- The wind regimes within the Lut Desert create an internal aeolian sediment-routing system
- The joint development of erosional and depositional landforms are consistent with modern sandflows
- Source-to-sink aeolian fluxes are of the same order of magnitude from decades to millions of years

Supporting Information:

Supporting Information may be found in the online version of this article.

Correspondence to:

L. Barrier,
barrier@ipgp.fr

Citation:

Chanteloube, C., Barrier, L., Derakhshani, R., Gadal, C., Braucher, R., Payet, V., et al. (2022). Source-to-sink aeolian fluxes from arid landscape dynamics in the Lut Desert. *Geophysical Research Letters*, *49*, e2021GL097342. https://doi.org/10.1029/2021GL097342

Received 3 DEC 2021
Accepted 30 JAN 2022

Author Contributions:

Conceptualization: Laurie Barrier, Clément Narteau
Formal analysis: Colin Chanteloube, Laurie Barrier, Vincent Payet, Clément Narteau
Funding acquisition: Laurie Barrier, Clément Narteau
Investigation: Reza Derakhshani, Régis Braucher, Laëtitia Léanni
Methodology: Colin Chanteloube, Laurie Barrier, Clément Narteau
Project Administration: Laurie Barrier
Software: Colin Chanteloube, Cyril Gadal
Supervision: Laurie Barrier, Clément Narteau
Visualization: Colin Chanteloube, Laurie Barrier, Clément Narteau
Writing – original draft: Colin Chanteloube, Laurie Barrier, Cyril Gadal, Régis Braucher, Clément Narteau

© 2022. American Geophysical Union. All Rights Reserved.

Source-To-Sink Aeolian Fluxes From Arid Landscape Dynamics in the Lut Desert

Colin Chanteloube[1], Laurie Barrier[1], Reza Derakhshani[2,3], Cyril Gadal[1], Régis Braucher[4], Vincent Payet[5], Laëtitia Léanni[4], and Clément Narteau[1]

[1]Université de Paris, Institut de physique du globe de Paris, CNRS, Paris, France, [2]Department of Geology, Shahid Bahonar University of Kerman, Kerman, Iran, [3]Department of Earth Sciences, Utrecht University, Utrecht, The Netherlands, [4]Aix-Marseille University, CNRS, IRD, Collège de France, INRAE, CEREGE, Aix-en-Provence, France, [5]Institut Pierre Simon Laplace, CNRS, Palaiseau, France

Abstract We analyze major landforms of the Lut Desert in Iran to provide a comprehensive source-to-sink picture of aeolian systems on time scales from decades to millions of years. We map the modern sandflows, along which we evaluate the volume and chronology associated with the excavation of mega-yardangs upwind and the formation of giant dunes downwind. Sediment discharges deduced from long-term erosion and deposition are of the same order of magnitude (10^5–10^6 m^3 yr^{-1}) as short-term and medium-term sand discharges derived from wind data and dune morphodynamics. At the scale of the internal aeolian sediment-routing system of the Lut, we establish an overall sediment budget constrained by the joint development of the erosional and depositional landforms. Our findings thus quantify the geomorphic controls of aeolian processes on arid landscapes at multiple length and time scales, while providing information on mass exchanges between continents and atmosphere.

Plain Language Summary Wind-blown sand and dust emissions shape singular landscapes in arid environments and globally impact climate, life, and human activities. Nevertheless, the contributions of aeolian processes to the evolution of continental surfaces and to their mass exchanges with oceans and the atmosphere are still subject to considerable uncertainties. Compared to sediment transport in rivers, this is because wind transport is not associated with a well-identified channel network that directly links sand and dust production (source) to accumulation (sink) areas. The Lut Desert in Iran is nested in a closed topographic depression which provides an appropriate context to investigate the work of the wind. Spectacular landforms called mega-yardangs and giant dunes are used together with modern wind data to map and quantify sandflows at different time scales. These sandflows are consistent with each other from decades to millions of years and allow to estimate the amount of sediments transported across the Lut Desert or emitted into the atmosphere. These estimates are not only important for the management of terrestrial drylands, but they can also provide information about the past evolution of planetary bodies dominated by aeolian processes such as Mars or Titan.

1. Introduction

An accurate quantification of aeolian sediment fluxes is crucial to improve our current understanding of the Earth system dynamics and manage the societal impact of sand transport and dust emissions (Alizadeh-Choobari et al., 2014a; Goudie, 2020; Jickells et al., 2005; Opp et al., 2021; Shao et al., 2011). Since extensive measurements are difficult to implement in the field, estimates of aeolian fluxes rely essentially on remote sensing data and transport laws that integrate a large number of parameters for the airflow and granular bed (Kok et al., 2012; Livingstone & Warren, 2019; Thomas, 2011). However, confronted with all the sources of natural variability (wind regime, air recirculation, grain-size distribution, soil composition, etc.), performing a complete mass balance of aeolian transport remains challenging. Here, we consider long time scales to smooth out such variability and integrate arid landscape dynamics into the assessment of aeolian mass transfers, from sediment sources to sediment sinks. Fluxes resulting from such temporal integration can then yield a sediment budget for wind-blown sediments, including the amount of dust deflated into the atmosphere at the scale of an entire desert.

Over the last two decades, source-to-sink studies have provided a wealth of information on fluvial-dominated landscapes and their response to tectonic, climatic, and biologic forcings (Allen, 2008, 2017; Bentley Sr et al., 2016; Sadler & Jerolmack, 2015; Sømme et al., 2009). All these studies document sediment pathways from

the upstream catchments to the downstream basins to estimate the impact of transport processes on landscape dynamics and the stratigraphic evolution of depositional areas. This approach is now expanding for a variety of morpho-sedimentary systems in glacial (Jaeger & Koppes, 2016), lacustrine (Bouton et al., 2020), submarine (Liu et al., 2016; Salles et al., 2018), and aeolian environments (Fitzsimmons et al., 2020; Nicoll et al., 2020; Shao et al., 2011), not only on Earth but also on other planetary bodies (Boazman et al., 2021; Day & Kocurek, 2016). However, works dedicated to aeolian-dominated landscapes often remain qualitative or limited to a single component of the sediment budget such as erosion or accumulation, dust or sand (East et al., 2015; McMillan & Schoenbohm, 2020; Pastore et al., 2021; Sun, 2002; Zender et al., 2004). Hence, the potential of source-to-sink methods is still to be exploited to bring new quantitative information on aeolian sediment-routing systems and associated landforms.

By describing sandflows throughout the Sahara, Wilson (1971) has established the basis for source-to-sink considerations and the analysis of landscape dynamics in aeolian environments. This pioneering work revealed that deflation can be on the same order of magnitude as river erosion. Nevertheless, since most sandflows eventually end up in a river or in the sea, it was impossible to balance the sediment budget on such a continental scale. In principle, smaller aeolian systems, as closed as possible, seem more appropriate to investigate sediment transport and morphogenic processes according to the local wind regimes. Taking advantage of new remote sensing imagery and dating techniques, together with more accurate wind data and a deeper understanding of dune dynamics, we focus here on the aeolian landforms of the Lut Desert (southeastern Iran) to provide additional observational and theoretical evidences on the impact of sandflows on landscape dynamics.

2. Aeolian Landscapes in the Lut Desert

The Lut Desert is located in an NNW-SSE-oriented endorheic watershed, about 300-km wide and 600-km long, surrounded by active tectonic and volcanic mountain ranges formed during the Cenozoic collision between Arabia and Eurasia (Figure 1a and Figure S1, Text S1 in Supporting Information S1; Allen et al., 2004; Walker et al., 2009). In its center, a sedimentary basin collects all the sediments transported by an internal river network since the Miocene (Dresch, 1968; Reyre & Mohafez, 1972). This area has a hyper-arid continental climate with mean annual rainfall of less than 20 mm yr^{-1} and temperatures of up to 50°C. From late winter to early spring, northerly or southerly storm winds prevail, driven by meridional pressure gradients (Figures S3–S5 in Supporting Information S1). In summer, diurnal variations in the thermal structure of the basin and the surrounding mountains generate strong north-northwesterly winds during the day and easterly katabatic winds at night. These strong seasonal winds and a sparse vegetation cover promote aeolian entrainment, sand transport, and dust emission, which are the main agents in shaping outstanding landscapes (Dresch, 1968; Gabriel, 1938; Hamidi et al., 2013; Maghsoudi, 2021; Rashki et al., 2021).

We first recognize these aeolian landscapes as an organized mosaic of erosional and depositional features (Figure 1a and Figure S1b in Supporting Information S1). West of the Lut Desert, different landforms are carved with an NNW-SSE orientation in the continental fined-grained deposits of the sedimentary basin. Among them, the most striking scenery is a 70-km-wide and 130-km-long field of mega-yardangs reaching heights of more than 80 m (Figure 1b). Another one, less obvious but larger, is a 90-km-wide and 250-km-long closed depression surrounded by a set of smaller hollows (Figure 1a). This major topographic depression has a maximum depth of more than 200 m and corresponds to an imbricated endorheic area surrounding the field of mega-yardangs. All these closed erosional features must be of aeolian origin because no other transport agent than the wind (e.g., gravity-driven mass wasting and water flow) could have evacuated the abraded material or the sediments accumulated by other surface processes during their excavation.

Within and downwind of the main depression, different dune systems develop (Figure 1a). Trains of barchan dunes composed of bright grains can locally emerge in the corridors between yardangs, where coarser and darker grains form an armor layer (Figure 1b). To the southeast, at the mouth of the yardang field, longitudinal dunes and transverse bedforms coexist with a direction of elongation and migration that regularly bend from southeast to east (Figure 1c). They eventually reach the southern edge of a sand sea of more than 13,000 km^2 that covers the eastern part of the Lut Desert. The centre of this sand sea is dominated by giant transverse dunes (>100 m in height and >2 km in wavelength) migrating toward north-northeast with superimposed bedforms of different sizes and orientations (Figure 1d). On the side of this field of giant dunes, a rare diversity of smaller bedforms

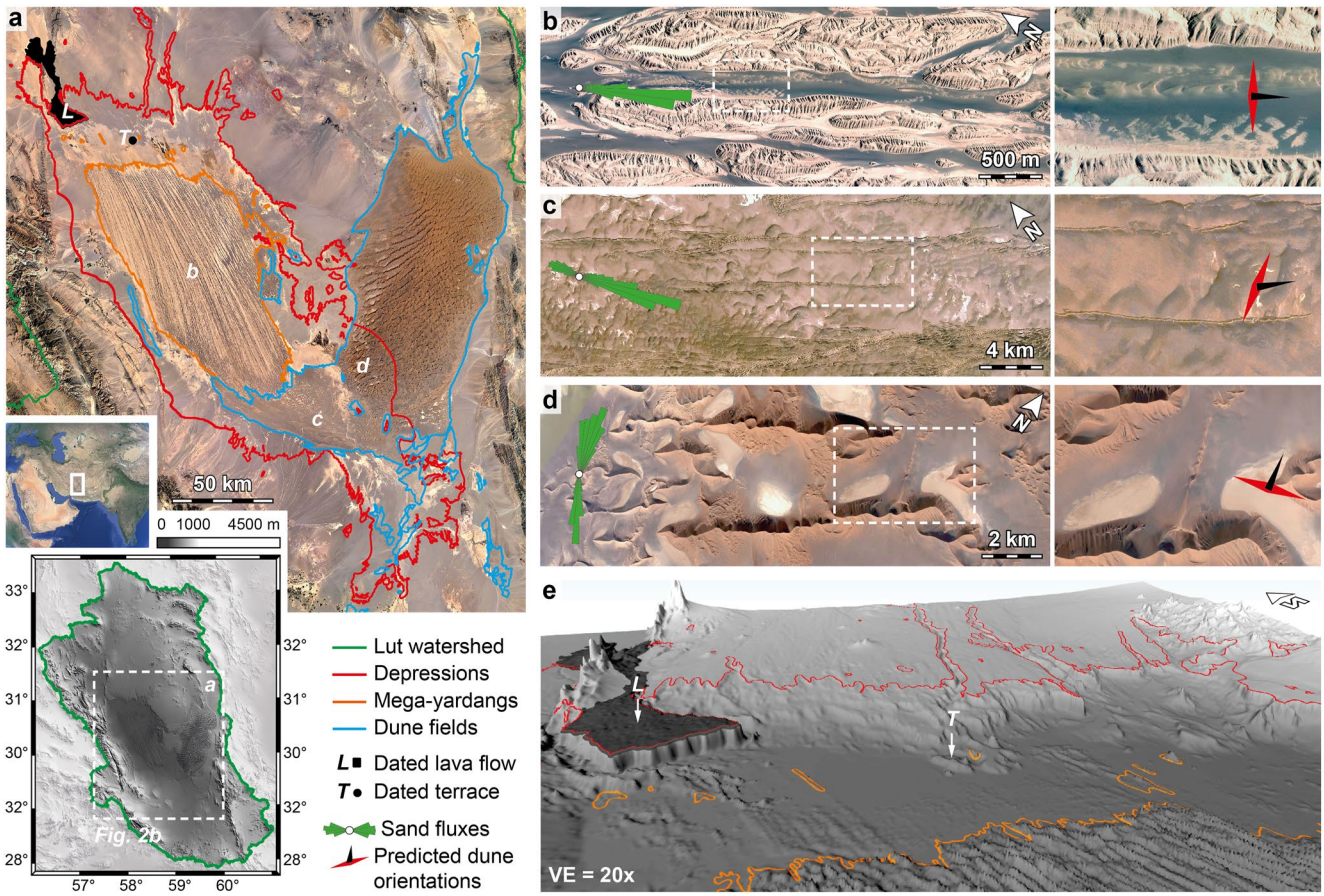


Figure 1. Aeolian landscapes of the Lut Desert. (a) Spatial organization of erosional (yardangs, depressions) and depositional (dune fields) landforms. (b) Mega-yardangs of 60-m high with trains of barchan dunes migrating on the armor layer of the inter-yardang corridors. (c) Coexistence of longitudinal and transverse bedforms downwind of the mega-yardang field. (d) Giant linear dunes within the sand sea. The sand flux roses and dune orientations are predicted from the ERA5-Land wind data. The double red and single black arrows correspond to the bed instability and elongating modes of dune growth, respectively. Images, roses, and arrows are rotated according to the main orientation of the local landforms. (e) 3D view of the northern edge of the main aeolian depression showing the dated Gandom Beryan lava flow (*L*) lying on top of the regional Mio-Pliocene sedimentary fill, and the dated terrace (*T*) at the edge of the main depression.

can be observed, including star, network, and barchanoid dunes. Further south, different dune fields of a few km^2 are scattered and grow from localized sediment sources associated with ephemeral rivers and playas. They are composed of migrating barchanoid and elongating linear dunes that all converge toward the sand sea.

3. Short-Term Transport Properties

We analyze the ERA5-Land surface wind data (Muñoz-Sabater et al., 2021) to describe the different wind regimes throughout the Lut Desert and map the corresponding aeolian transport routes over the last decades (Figure 2 and Figures S3–S13, Text S2 in Supporting Information S1). Mean potential sandflows are the streamlines derived from the resultant transport vector field (Fryberger & Dean, 1979; Pearce & Walker, 2005; Tsoar, 2005; Ungar & Haff, 1987). Considering a flat sand bed of similar grain size, each vector is computed as the sum of the saturated sand flux vectors derived from local wind data from 1979 to 2019. Thus, the mean potential sandflows display the resultant drift potential (RDP) and resultant drift direction (RDD) across the whole area (Figure 2a). Over the endorheic watershed, sandflows are mainly south-southeastwards. Then, they roll up counter-clockwise into a vortex spiral located above the center of the desert. These converging sandflows form an internal aeolian sediment-routing system, turning the Lut region into a major sand trap. In this routing system, the resultant transport is maximum at the upwind edge of the main aeolian depression. It remains high above the field of mega-yardangs and decreases significantly above the field of giant dunes to eventually fall to zero toward the center of the desert (Figure 2a). All areas are exposed to sand-transporting winds of similar strength blowing at different times of the

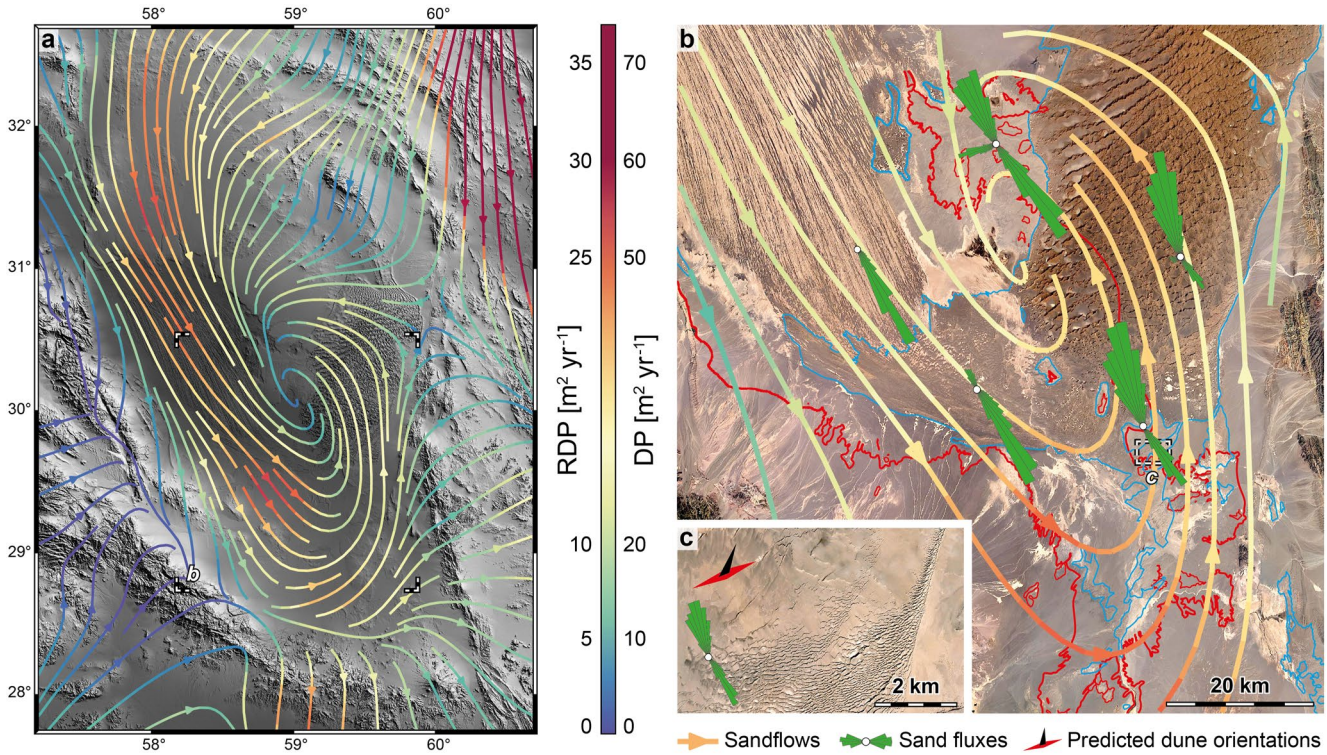


Figure 2. Modern aeolian transport routes in the Lut Desert. (a) Sandflows predicted from the ERA5-Land wind data. (b) A zoom in on the aeolian sediment-routing system from erosional to depositional landforms (red and blue outlines, respectively). Colors in (a) and (b) show the magnitude of the resultant drift potential (RDP) and drift potential (DP), respectively. While RDP varies along the sandflow paths, DP, which does not account for flux orientation, keeps a rather constant value. This illustrates a continuous transition from unidirectional to multidirectional wind regimes (see also sand flux roses). (c) Example of elongating and migrating dunes converging to the sand sea in a zone of low sand availability.

years, so that the convergent cyclonic transport pattern reflects a continuous transition from unimodal to more complex wind regimes along the sandflow paths (Figure 2b). This transition is evidenced by the different types of active bedforms (Gao, Narteau, Rozier & Courrech du Pont, 2015; Wasson & Hyde, 1983), from trains of barchan dunes between yardangs to longitudinal, reversing, and finally star dunes where the resultant sand flux drops (Figures 2b and 2c). Locally, the divergence of sandflows gives short-term erosion and deposition rates of the order of 0.1 mm yr^{-1} (Figure S10 in Supporting Information S1). Integrating sandflows perpendicularly to the transport direction downwind of the mega-yardang field and upwind of the sand sea, we estimate output and input discharges of 0.8×10^6 and 0.4×10^6 m^3 yr^{-1} over the last 40 years (Figure S14, Text S3 in Supporting Information S1).

4. Long-Term Transport Properties

Based on morpho-sedimentary mapping (Figure 1, Figures S1b and S15a in Supporting Information S1), we characterize the spatial and chronological organization of the aeolian landforms of the Lut Desert to quantify their combined dynamics over the last million years (Figure 3 and Figures S15–S20, Text S4 in Supporting Information S1). For erosional landforms, we assess the volume of sediments excavated from the aeolian depressions using the top surface of the sedimentary fill of the basin. Lying on this surface and cross-cut by the north-east border of the main depression, the Gandom Beryan lava flow was emplaced at the transition between the end of the basin filling and the onset of aeolian erosion (Figures 1a, 1e and Figure S20 in Supporting Information S1). This basaltic flow is dated to 2.35 ± 0.22 Ma by radiometric analyses (Walker et al., 2009), which sets a maximum incision age for the aeolian depressions and yardangs throughout the region. At the edge of the main depression, a lower terrace is also dated by cosmogenic isotope analyses giving a minimum exposure age of 109 ± 17 ka for its gravel pavement (Figures 1a, 1e and Figures S17, S19 in Supporting Information S1). Considering the relics of the two dated surfaces, a range of paleotopographies can be reconstructed across the entire area

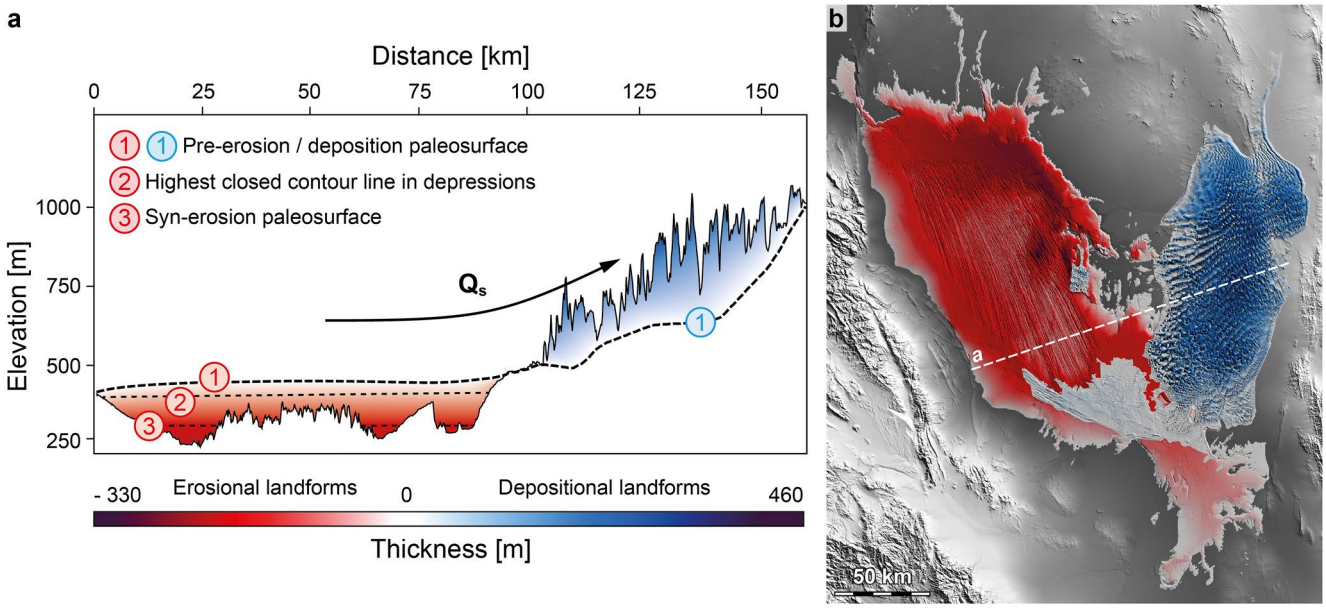


Figure 3. Long-term erosion and deposition from the aeolian landscapes of the Lut Desert. (a) Cross-section of the present-day topography and paleosurface reconstructions. In contrast with fluvial-dominated landscapes, aeolian deposition can occur up the slope, at higher elevation than aeolian erosion. (b) Map view of the sediment thicknesses excavated from erosional landforms (yardangs and depressions) and accumulated in depositional landforms (dune fields).

(Figure 3a, Figures S15c, and S15d in Supporting Information S1). Subtracting the current topography from the reconstructed ones, we obtain excavated sediment volumes of 1,500 and 130 km^3 since the early Quaternary and late Pleistocene, respectively (Figure 3b). For depositional landforms, we measure the volume of sand accumulated within the different dune systems. Since they drape the top surface of the basin fill and the bottom of the main depression, their formation must be synchronous or posterior to the onset of aeolian erosion. The basal surface on which dunes have grown can be reconstructed from the topography of the bedrock outcrops around and within the sand sea (Figure 3a and Figure S15d in Supporting Information S1). The difference in altitude between the current topography and this basal surface shows that a volume of 890 km^3 of aeolian deposits have accumulated in the form of dunes during the Quaternary (Figure 3b). All these volumetric reconstructions and their time constraints give long-term erosion and deposition rates of the order of 0.1 mm yr^{-1}. From the material excavated from the depressions, we estimate erosion discharges of 0.6×10^6 and 1.2×10^6 m^3 yr^{-1} over the past 2.35 Myr and 109 kyr, respectively. From the sand captured in the dune fields, a deposition discharge of 0.4×10^6 m^3 yr^{-1} is also assessed over the past 2.35 Myr.

5. Discussion and Conclusions

Our results offer a comprehensive quantitative picture of the aeolian sediment-routing system that has shaped the landscapes of the Lut Desert. These Quaternary features cover areas that geographically coincide perfectly with the geometry of the present-day transport pathways (Figure S13 in Supporting Information S1). Sandflows derived from modern wind data are sufficient to explain the exchange of mass from aeolian depressions to dune fields (Figure 2), providing a coherent scenario for the long-term spatial organization and temporal evolution of these landforms (Figure 3). In addition, the sand discharges integrated downwind of the depressions and upwind of the sand sea over climatic time scales are not only of the same order of magnitude, but also consistent with the erosion and deposition discharges deduced over geological time scales from the volumetric reconstructions (Figure 4). Eventually, bedform alignments predicted from the wind data are in agreement with the observed dune orientations (Figures 1, 2 and Figures S12–S13, Text S3 in Supporting Information S1), which suggests a stability of wind regimes and transport properties over the intermediate time scales from centuries to millennia associated with dune growth and migration (Figure 4).

According to its definition, the mean potential sandflows are an upper limit of aeolian transport considering a flat bed of loose sand of homogeneous grain size (Ungar & Haff, 1987). Such a condition is rarely met in the

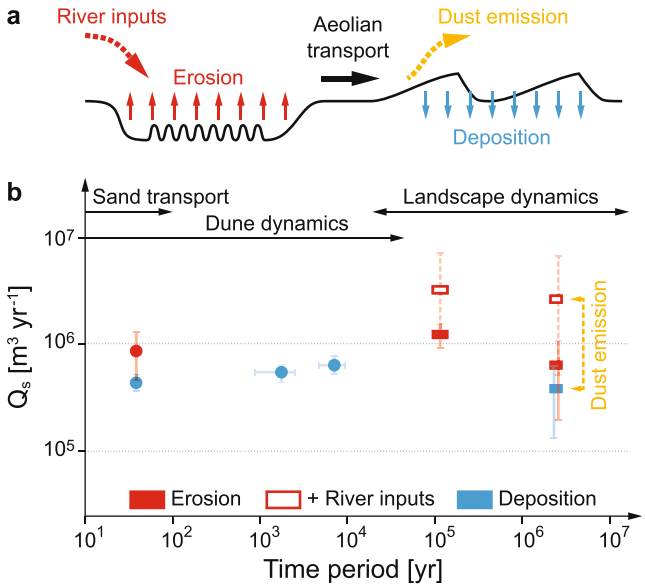


Figure 4. Persistent contribution of aeolian processes to the landscapes dynamics of the Lut Desert. (a) Schematic representation of the mass exchange processes in the endorheic watershed of the Lut Desert. (b) Sediment discharges averaged over different time scales, from short-term transport properties (decades) to long-term landscape dynamics (tens of thousands to millions of years). Giant dune patterns provide information over intermediate time scales (centuries to millennia) thanks to their characteristic growth time and the sand fluxes associated with their migration or elongation (Text S3 in Supporting Information S1). Discharges in $m^3\ yr^{-1}$ can be converted into loads in $t\ yr^{-1}$ by multiplying them by the mean density of the sediment grains, which is typically 2.6.

Lut Desert, especially in the area connecting the erosional and depositional landforms. Instead, these buffer zones are characterized by an alternation of elongating dunes, evaporitic deposits, and gravelly surfaces of alluvial fans (Figures 1 and 3). While the saturated flux cannot be reached on the cohesive upper layer of these sedimentary soils, what could appear to be a deficit of sand flux in our predictions may be compensated by the wind speed-up on the stoss slopes of elongating dunes (Gao et al., 2021; Lucas et al., 2015). Indeed, as these dunes form under winds that alternatively blow from both sides of their crests, they enhance transport on their flanks in the direction along which they elongate (Courrech du Pont et al., 2014). Thus, fields of elongating dunes can efficiently accommodate high and low resultant transport by adapting their width and spacing (Wasson & Hyde, 1983). Hence, they can have evolved over time to transfer sediments from the main depression to the sand sea depending on climatic conditions and sediment availability. Another fundamental property of elongating dunes is that they do not behave like sediment traps. They develop by losing sand in the direction of the prevailing winds (Rozier et al., 2019), so that the interdune areas are continuously exposed to sand fluxes originating from the lee slopes. On the sedimentary soils of the Lut watershed, these free fluxes can cause dust emission over distances of up to 100 km from the field of mega-yardangs to the sand sea.

Our estimates show that dune fields represent only a fraction of the volume excavated by the wind from erosional depressions (Figure 4). This fraction is even lower if we consider the material brought in these endorheic features by the surrounding dryland river system during their incision. Based on denudation rates measured in arid climates, this contribution could correspond to a median discharge of $2 \times 10^6\ m^3\ yr^{-1}$ (Figure 4 and Table S10 in Supporting Information S1). Consequently, only a fraction of the wind-blown particles have accumulated in dune fields since the onset of aeolian erosion. As there is no evidence of sand evacuation through the mountain ranges surrounding the Lut watershed, the difference corresponds to the emission of dust into the atmosphere, which could represent a discharge of $2.2 \times 10^6\ m^3\ yr^{-1}$. Accordingly, the Lut Desert is not only an internal aeolian routing system for sand (Wilson, 1971), it is also a major source of atmospheric dust leading to an overall loss of mass at the scale of this endorheic region.

Performed in a hyper-arid environment, this sediment budget underpins our knowledge on the morphodynamics of aeolian systems at multiple space and time scales. It shows that a source-to-sink approach can be used to assess mass exchanges on continental surfaces, but also with the atmosphere. A significant contribution of dust emission to the overall budget can indeed be achieved when considering the fine grain sizes of the eroded material, as well as the numbers of seasonal cycles and transport events required for mass transfer in multidirectional wind regimes. Besides this contribution, we demonstrate that wind-blown sand plays a prominent and persistent role in shaping arid landscapes, whether by erosion or deposition. These morphogenic processes now need to be analyzed according to climate cycles and the variability of aeolian transport, both in aeolian sand-routing systems and in dust deposition areas. At this stage, our evaluations cannot distinguish significant changes in aeolian transport during interglacial and glacial periods. Additional works are thus required to account for any fluctuations around the mean discharges that we are now able to provide. They should help to determine soil properties and sand availability as a function of aridity conditions, as well as wind strength in mid-latitude continental regions during the Quaternary.

Given the extent of terrestrial drylands, hot or cold, our quantitative results reveal the full potential of source-to-sink methods to document how aeolian processes drive landscape dynamics and closely link the evolution of continental surfaces to atmospheric circulations. Except for dating, similar studies can also be implemented on other aeolian-dominated planetary surfaces of the solar system. They will translate into new research oppor-

tunities, notably to decipher modern and past climatic conditions on Earth, Mars, or Titan from the feedbacks between aerodynamics, granular mechanics, and landscape dynamics.

Data Availability Statement

Supporting text, figures, and tables, as well as information on the data used in this study, can be found in Supporting Information. The ERA5-Land reanalysis data are hosted on the ECMWF website (https://cds.climate.copernicus.eu/cdsapp#!/dataset/reanalysis-era5-land?tab=overview). The Landsat, Sentinel, SPOT, Pleiades, and DigitalGlobe satellite images are available through the Google Earth Engine (https://www.google.com/earth/download/gep/agree.html). The digital elevation models SRTM30, SRTM3, and AW3D30 can be retrieved through the EarthExplorer user interface developed by the USGS (https://earthexplorer.usgs.gov) and ALOS Global DSM portal (https://www.eorc.jaxa.jp/ALOS/en/dataset/aw3d30/aw3d30_e.htm), respectively. Figures are generated with Python 3.9, Global Mapper 21.1, and Adobe Illustrator 2020.

Acknowledgments
The authors acknowledge financial support from the UnivEarthS LabEx program (ANR-10-LABX-0023), the IdEx Université de Paris (ANR-18-IDEX-0001), the IPGP BQR and CNRS-INSU SYSTER programs, the French National Research Agency (ANR-17-CE01-0014), the National Science Center of Poland (Grant 2016/23/B/ST10/01700), and the French Chinese International laboratory SALADYN. The ASTER AMS national facility (CEREGE, Aix-en-Provence) is supported by the INSU-CNRS, the IRD, and the ANR through the "Projets thématiques d'excellence" program for the "Equipements d'excellence" ASTER-CEREGE action. The ASTER Team (Aumaître G., Bourlès D.L., and K. Keddadouche) are thanked for, their expertise in AMS. We also thank Paul Kapp and an anonymous reviewer for their careful reading of our manuscript and their insightful comments and suggestions. This publication is IPGP contribution #4252. It contains modified Copernicus Climate Change Service Information (2020). Neither the European Commission nor ECMWF is responsible for any use that may be made of the Copernicus Information or Data it contains.

References

Aguilar, G., Carretier, S., Regard, V., Vassallo, R., Riquelme, R., & Martinod, J. (2014). Grain size-dependent ^{10}Be concentrations in alluvial stream sediment of the Huasco Valley, a semi-arid Andes region. *Quaternary Geochronology*, *19*, 163–172. https://doi.org/10.1016/j.quageo.2013.01.011

Al-Dousari, A., Al-Enezi, A., & Al-Awadhi, J. (2008). Textural variations within different representative types of dune sediments in Kuwait. *Arabian Journal of Geosciences*, *1*(1), 17–31. https://doi.org/10.1007/s12517-008-0002-4

Alizadeh-Choobari, O., Zawar-Reza, P., & Sturman, A. (2014a). The global distribution of mineral dust and its impacts on the climate system: A review. *Atmospheric Research*, *138*, 152–165. https://doi.org/10.1016/j.atmosres.2013.11.007

Alizadeh-Choobari, O., Zawar-Reza, P., & Sturman, A. (2014b). The "wind of 120 days" and dust storm activity over the Sistan Basin. *Atmospheric Research*, *143*, 328–341. https://doi.org/10.1016/j.atmosres.2014.02.001

Allen, M., Jackson, J., & Walker, R. (2004). Late Cenozoic reorganization of the Arabia-Eurasia collision and the comparison of short-term and long-term deformation rates. *Tectonics*, *23*(2). https://doi.org/10.1029/2003tc001530

Allen, P. A. (2008). From landscapes into geological history. *Nature*, *451*(7176), 274–276. https://doi.org/10.1038/nature06586

Allen, P. A. (2017). *Sediment routing systems: The fate of sediment from source to sink*. Cambridge University Press.

Bagnold, R. A. (1941). *The physics of wind blown sand and desert dunes*. Methuen.

Bentley Sr, S., Blum, M., Maloney, J., Pond, L., & Paulsell, R. (2016). The Mississippi River source-to-sink system: Perspectives on tectonic, climatic, and anthropogenic influences, Miocene to Anthropocene. *Earth-Science Reviews*, *153*, 139–174. https://doi.org/10.1016/j.earscirev.2015.11.001

Boazman, S., Davis, J., Grindrod, P., Balme, M., Vermeesch, P., & Baird, T. (2021). Measuring ripple and dune migration in Coprates Chasma, Valles Marineris: A source to sink aeolian system on Mars? *Journal of Geophysical Research: Planets*, e2020JE006608.

Borchers, B., Marrero, S., Balco, G., Caffee, M., Goehring, B., Lifton, N., et al. (2016). Geological calibration of spallation production rates in the CRONUS-Earth project. *Quaternary Geochronology*, *31*, 188–198. https://doi.org/10.1016/j.quageo.2015.01.009

Bouton, A., Vennin, E., Amiotte-Suchet, P., Thomazo, C., Sizun, J.-P., Virgone, A., et al. (2020). Prediction of the calcium carbonate budget in a sedimentary basin: A "source-to-sink" approach applied to Great Salt Lake, Utah, USA. *Basin Research*, *32*(5), 1015–1044. https://doi.org/10.1111/bre.12412

Braucher, R., Guillou, V., Bourlès, D., Arnold, M., Aumaître, G., Keddadouche, K., et al. (2015). Preparation of ASTER in-house ^{10}Be/^{9}Be standard solutions. *Nuclear Instruments and Methods in Physics Research Section B: Beam Interactions with Materials and Atoms*, *361*, 335–340. https://doi.org/10.1016/j.nimb.2015.06.012

Braucher, R., Matmon, A., Bourlès, D., Aumaître, G., & Keddadouche, K. (2019). Towards successful cleaning of chert samples for improved ^{10}Be and ^{26}Al measurements. *Nuclear Instruments and Methods in Physics Research Section B: Beam Interactions with Materials and Atoms*, *456*, 257–263.

Braucher, R., Merchel, S., Borgomano, J., & Bourlès, D. (2011). Production of cosmogenic radionuclides at great depth: A multi element approach. *Earth and Planetary Science Letters*, *309*(1–2), 1–9. https://doi.org/10.1016/j.epsl.2011.06.036

Britter, R., Hunt, J., & Richards, K. (1981). Air flow over a two-dimensional hill: Studies of velocity speed-up, roughness effects and turbulence. *Quarterly Journal of the Royal Meteorological Society*, *107*(451), 91–110. https://doi.org/10.1002/qj.49710745106

Carretier, S., Regard, V., Vassallo, R., Aguilar, G., Martinod, J., Riquelme, R., et al. (2013). Slope and climate variability control of erosion in the Andes of central Chile. *Geology*, *41*(2), 195–198. https://doi.org/10.1130/g33735.1

Carretier, S., Regard, V., Vassallo, R., Aguilar, G., Martinod, J., Riquelme, R., et al. (2015). Differences in ^{10}Be concentrations between river sand, gravel and pebbles along the western side of the central Andes. *Quaternary Geochronology*, *27*, 33–51. https://doi.org/10.1016/j.quageo.2014.12.002

Chmeleff, J., von Blanckenburg, F., Kossert, K., & Jakob, D. (2010). Determination of the ^{10}Be half-life by multicollector ICP-MS and liquid scintillation counting. *Nuclear Instruments and Methods in Physics Research Section B: Beam Interactions with Materials and Atoms*, *268*(2), 192–199. https://doi.org/10.1016/j.nimb.2009.09.012

Clapp, E. M., Bierman, P. R., Schick, A. P., Lekach, J., Enzel, Y., & Caffee, M. (2000). Sediment yield exceeds sediment production in arid region drainage basins. *Geology*, *28*(11), 995–998. https://doi.org/10.1130/0091-7613(2000)028<0995:syespi>2.3.co;2

Cockburn, H. A., Seidl, M. A., & Summerfield, M. A. (1999). Quantifying denudation rates on inselbergs in the central Namib Desert using in situ–produced cosmogenic ^{10}Be and ^{26}Al. *Geology*, *27*(5), 399–402. https://doi.org/10.1130/0091-7613(1999)027<0399:qdroii>2.3.co;2

Conrad, G., Montigny, R., Thuizat, R., & Westphal, M. (1981). Tertiary and Quaternary geodynamics of southern Lut (Iran) as deduced from palaeomagnetic, isotopic and structural data. *Tectonophysics*, *75*(3–4), T11–T17. https://doi.org/10.1016/0040-1951(81)90272-9

Courrech du Pont, S., Narteau, C., & Gao, X. (2014). Two modes for dune orientation. *Geology*, *42*(9), 743–746. https://doi.org/10.1130/g35657.1

Day, M., & Kocurek, G. (2016). Observations of an aeolian landscape: From surface to orbit in Gale Crater. *Icarus*, *280*, 37–71. https://doi.org/10.1016/j.icarus.2015.09.042

Dickinson, W. W., & Ward, J. D. (1994). Low depositional porosity in eolian sands and sandstones, Namib Desert. *Journal of Sedimentary Research*, *64*(2a), 226–232. https://doi.org/10.1306/d4267d66-2b26-11d7-8648000102c1865d

Dresch, J. (1968). Reconnaissance dans le Lut (Iran). *Bulletin de l'Association de Geographes Français*, *45*(362), 143–153. https://doi.org/10.3406/bagf.1968.5869

Dunai, T. J., López, G. A. G., & Juez-Larré, J. (2005). Oligocene–Miocene age of aridity in the Atacama Desert revealed by exposure dating of erosion-sensitive landforms. *Geology*, *33*(4), 321–324. https://doi.org/10.1130/g21184.1

Durán, O., Claudin, P., & Andreotti, B. (2011). On aeolian transport: Grain-scale interactions, dynamical mechanisms and scaling laws. *Aeolian Research*, *3*(3), 243–270. https://doi.org/10.1016/j.aeolia.2011.07.006

East, A. E., Clift, P. D., Carter, A., Alizai, A., & VanLaningham, S. (2015). Fluvial–eolian interactions in sediment routing and sedimentary signal buffering: An example from the Indus Basin and Thar Desert. *Journal of Sedimentary Research*, *85*(6), 715–728. https://doi.org/10.2110/jsr.2015.42

Elbelrhiti, H., Claudin, P., & Andreotti, B. (2005). Field evidence for surface-wave-induced instability of sand dunes. *Nature*, *437*, 720–723. https://doi.org/10.1038/nature04058

Elkhrachy, I. (2018). Vertical accuracy assessment for SRTM and ASTER Digital Elevation Models: A case study of Najran city, Saudi Arabia. *Ain Shams Engineering Journal*, *9*(4), 1807–1817. https://doi.org/10.1016/j.asej.2017.01.007

Ewing, R. C., & Kocurek, G. A. (2010). Aeolian dune interactions and dune-field pattern formation: White Sands Dune Field, New Mexico. *Sedimentology*, *57*(5), 1199–1219. https://doi.org/10.1111/j.1365-3091.2009.01143.x

Ewing, R. C., McDonald, G. D., & Hayes, A. G. (2015). Multi-spatial analysis of aeolian dune-field patterns. *Geomorphology*, *240*, 44–53. https://doi.org/10.1016/j.geomorph.2014.11.023

Farr, T. G., Rosen, P. A., Caro, E., Crippen, R., Duren, R., Hensley, S., et al. (2007). The shuttle radar topography mission. *Reviews of Geophysics*, *45*(2). https://doi.org/10.1029/2005rg000183

Fernandez-Cascales, L., Lucas, A., Rodriguez, S., Gao, X., Spiga, A., & Narteau, C. (2018). First quantification of relationship between dune orientation and sediment availability, Olympia Undae, Mars. *Earth and Planetary Science Letters*, *489*, 241–250. https://doi.org/10.1016/j.epsl.2018.03.001

Field, J., & Pelletier, J. (2018). Controls on the aerodynamic roughness length and the grain-size dependence of aeolian sediment transport. *Earth Surface Processes and Landforms*, *43*, 2616–2626. https://doi.org/10.1002/esp.4420

Fitzsimmons, K. E., Nowatzki, M., Dave, A. K., & Harder, H. (2020). Intersections between wind regimes, topography and sediment supply: Perspectives from aeolian landforms in Central Asia. *Palaeogeography, Palaeoclimatology, Palaeoecology*, *540*, 109531. https://doi.org/10.1016/j.palaeo.2019.109531

Fryberger, S. G., & Dean, G. (1979). Dune forms and wind regime. In *A study of global sand seas* (Vol. 1052, pp. 137–169). US Government Printing Office Washington.

Gabriel, A. (1938). The southern Lut and Iranian Baluchistan. *The Geographical Journal*, *92*(3), 193–208. https://doi.org/10.2307/1788828

Gao, X., Narteau, C., & Gadal, C. (2021). Migration of reversing dunes against the sand flow path as a singular expression of the speed-up effect. *Journal of Geophysical Research: Earth Surface*, *126*(5), e2020JF005913. https://doi.org/10.1029/2020jf005913

Gao, X., Narteau, C., & Rozier, O. (2015). Development and steady states of transverse dunes: A numerical analysis of dune pattern coarsening and giant dunes. *Journal of Geophysical Research: Earth Surface*, *120*, 2200–2219. https://doi.org/10.1002/2015JF003549

Gao, X., Narteau, C., Rozier, O., & Courrech du Pont, S. (2015). Phase diagrams of dune shape and orientation depending on sand availability. *Scientific Reports*, *5*(1), 1–12. https://doi.org/10.1038/srep14677

Goudie, A. S. (2020). Dust storms and human health. In *Extreme weather events and human health* (pp. 13–24). Springer. https://doi.org/10.1007/978-3-030-23773-8_2

Hamidi, M., Kavianpour, M. R., & Shao, Y. (2013). Synoptic analysis of dust storms in the Middle East. *Asia-Pacific Journal of Atmospheric Sciences*, *49*(3), 279–286. https://doi.org/10.1007/s13143-013-0027-9

Harel, M.-A., Mudd, S., & Attal, M. (2016). Global analysis of the stream power law parameters based on worldwide ^{10}Be denudation rates. *Geomorphology*, *268*, 184–196. https://doi.org/10.1016/j.geomorph.2016.05.035

Iversen, J. D., Greeley, R., Marshall, J. R., & Pollack, J. B. (1987). Aeolian saltation threshold: The effect of density ratio. *Sedimentology*, *34*(4), 699–706. https://doi.org/10.1111/j.1365-3091.1987.tb00795.x

Jackson, P. S., & Hunt, J. C. R. (1975). Turbulent wind flow over a low hill. *Quarterly Journal of the Royal Meteorological Society*, *101*, 929–955. https://doi.org/10.1002/qj.49710143015

Jaeger, J. M., & Koppes, M. N. (2016). The role of the cryosphere in source-to-sink systems. *Earth-Science Reviews*, *153*, 43–76. https://doi.org/10.1016/j.earscirev.2015.09.011

Jayko, A. (2005). Late Quaternary denudation, Death and Panamint valleys, eastern California. *Earth-Science Reviews*, *73*(1–4), 271–289. https://doi.org/10.1016/j.earscirev.2005.04.009

Jickells, T., An, Z., Andersen, K. K., Baker, A., Bergametti, G., Brooks, N., et al. (2005). Global iron connections between desert dust, ocean biogeochemistry, and climate. *Science*, *308*(5718), 67–71. https://doi.org/10.1126/science.1105959

Johnson, K. S. (1997). Evaporite karst in the United States. *Carbonates and Evaporites*, *12*(1), 2–14. https://doi.org/10.1007/bf03175797

Jolivet, M., Braucher, R., Dovchintseren, D., Hocquet, S., Schmitt, J.-M., Team, A., et al. (2021). Erosion around a large-scale topographic high in a semi-arid sedimentary basin: Interactions between fluvial erosion, aeolian erosion and aeolian transport. *Geomorphology*, *386*, 107747. https://doi.org/10.1016/j.geomorph.2021.107747

Kapp, P., Pelletier, J. D., Rohrmann, A., Heermance, R., Russell, J., Ding, L., et al. (2011). Wind erosion in the Qaidam basin, central Asia: Implications for tectonics, paleoclimate, and the source of the Loess Plateau. *Geological Society of America Today*, *21*(4/5), 4–10. https://doi.org/10.1130/gsatg99a.1

Kober, F., Ivy-Ochs, S., Schlunegger, F., Baur, H., Kubik, P., & Wieler, R. (2007). Denudation rates and a topography-driven rainfall threshold in northern Chile: Multiple cosmogenic nuclide data and sediment yield budgets. *Geomorphology*, *83*(1–2), 97–120. https://doi.org/10.1016/j.geomorph.2006.06.029

Kober, F., Ivy-Ochs, S., Zeilinger, G., Schlunegger, F., Kubik, P. W., Baur, H., et al. (2009). Complex multiple cosmogenic nuclide concentration and histories in the arid Rio Lluta catchment, northern Chile. *Earth Surface Processes and Landforms*, *34*(3), 398–412. https://doi.org/10.1002/esp.1748

Kok, J. F., Parteli, E. J., Michaels, T. I., & Karam, D. B. (2012). The physics of wind-blown sand and dust. *Reports on Progress in Physics*, *75*(10), 106901. https://doi.org/10.1088/0034-4885/75/10/106901

Korschinek, G., Bergmaier, A., Faestermann, T., Gerstmann, U., Knie, K., Rugel, G., et al. (2010). A new value for the half-life of ^{10}Be by heavy-ion elastic recoil detection and liquid scintillation counting. *Nuclear Instruments and Methods in Physics Research Section B: Beam Interactions with Materials and Atoms*, *268*(2), 187–191. https://doi.org/10.1016/j.nimb.2009.09.020

Lal, D. (1991). Cosmic ray labeling of erosion surfaces: In situ nuclide production rates and erosion models. *Earth and Planetary Science Letters*, *104*(2–4), 424–439. https://doi.org/10.1016/0012-821x(91)90220-c

Laurent, B., Marticorena, B., Bergametti, G., Chazette, P., Maignan, F., & Schmechtig, C. (2005). Simulation of the mineral dust emission frequencies from desert areas of China and Mongolia using an aerodynamic roughness length map derived from the POLDER/ADEOS 1 surface products. *Journal of Geophysical Research: Atmospheres*, *110*(D18). https://doi.org/10.1029/2004jd005013

Liu, Z., Zhao, Y., Colin, C., Stattegger, K., Wiesner, M. G., Huh, C.-A., et al. (2016). Source-to-sink transport processes of fluvial sediments in the south China sea. *Earth-Science Reviews*, *153*, 238–273. https://doi.org/10.1016/j.earscirev.2015.08.005

Livingstone, I. (1987). Grain-size variation on a 'complex' linear dune in the Namib Desert. *Geological Society, London, Special Publications*, *35*(1), 281–291. https://doi.org/10.1144/gsl.sp.1987.035.01.19

Livingstone, I., & Warren, A. (2019). *Aeolian geomorphology: A new introduction*. John Wiley & Sons.

Lü, P., Narteau, C., Dong, Z., Claudin, P., Rodriguez, S., An, Z., et al. (2021). Direct validation of dune instability theory. *Proceedings of the National Academy of Sciences*, *118*(17). https://doi.org/10.1073/pnas.2024105118

Lü, P., Narteau, C., Dong, Z., Rozier, O., & Courrech Du Pont, S. (2017). Unravelling raked linear dunes to explain the coexistence of bedforms in complex dunefields. *Nature Communications*, *8*, 14239. https://doi.org/10.1038/ncomms14239

Lucas, A., Narteau, C., Rodriguez, S., Rozier, O., Callot, Y., Garcia, A., et al. (2015). Sediment flux from the morphodynamics of elongating linear dunes. *Geology*, *43*(11), 1027–1030. https://doi.org/10.1130/g37101.1

Maghsoudi, M. (2021). *Desert landscapes and landforms of Iran*. Springer Nature.

Marticorena, B., Chazette, P., Bergametti, G., Dulac, F., & Legrand, M. (2004). Mapping the aerodynamic roughness length of desert surfaces from the POLDER/ADEOS bi-directional reflectance product. *International Journal of Remote Sensing*, *25*(3), 603–626. https://doi.org/10.1080/0143116031000116976

Matmon, A., Simhai, O., Amit, R., Haviv, I., Porat, N., McDonald, E., et al. (2009). Desert pavement–coated surfaces in extreme deserts present the longest-lived landforms on Earth. *The Geological Society of America Bulletin*, *121*(5–6), 688–697. https://doi.org/10.1130/b26422.1

McMillan, M., & Schoenbohm, L. M. (2020). Large-scale Cenozoic Wind Erosion in the Puna Plateau: The Salina del Fraile Depression. *Journal of Geophysical Research: Earth Surface*, *125*(9), e2020JF005682. https://doi.org/10.1029/2020jf005682

McPhillips, D., Bierman, P. R., Crocker, T., & Rood, D. H. (2013). Landscape response to Pleistocene-Holocene precipitation change in the Western Cordillera, Peru: 10Be concentrations in modern sediments and terrace fills. *Journal of Geophysical Research: Earth Surface*, *118*(4), 2488–2499. https://doi.org/10.1002/2013jf002837

Merchel, S., & Bremser, W. (2004). First international ^{26}Al interlaboratory comparison—Part I. *Nuclear Instruments and Methods in Physics Research Section B: Beam Interactions with Materials and Atoms*, *223*, 393–400. https://doi.org/10.1016/j.nimb.2004.04.076

Morris, D. A., & Johnson, A. I. (1967). *Summary of hydrologic and physical properties of rock and soil materials, as analyzed by the hydrologic laboratory of the US Geological Survey, 1948-60* (Tech. Rep.). US Government Printing Office

Muñoz Sabater, J. (2019). *ERA5-Land hourly data from 1981 to present*. Copernicus Climate Change Service (C3S) Climate Data Store (CDS).

Muñoz-Sabater, J., Dutra, E., Agustí-Panareda, A., Albergel, C., Arduini, G., Balsamo, G., et al. (2021). ERA5-Land: A state-of-the-art global reanalysis dataset for land applications. *Earth System Science Data Discussions*, 1–50. https://doi.org/10.5194/essd-13-4349-2021

Narteau, C., Zhang, D., Rozier, O., & Claudin, P. (2009). Setting the length and time scales of a cellular automaton dune model from the analysis of superimposed bed forms. *Journal of Geophysical Research: Earth Surface*, *114*, F03006. https://doi.org/10.1029/2008JF001127

Nicoll, K., Hahnenberger, M., & Goldstein, H. L. (2020). 'Dust in the wind' from source-to-sink: Analysis of the 14–15 April 2015 storm in Utah. *Aeolian Research*, *46*, 100532. https://doi.org/10.1016/j.aeolia.2019.06.002

Nishiizumi, K. (2004). Preparation of ^{26}Al AMS standards. *Nuclear Instruments and Methods in Physics Research Section B: Beam Interactions with Materials and Atoms*, *223*, 388–392. https://doi.org/10.1016/j.nimb.2004.04.075

Nishiizumi, K., Imamura, M., Caffee, M. W., Southon, J. R., Finkel, R. C., & McAninch, J. (2007). Absolute calibration of ^{10}Be AMS standards. *Nuclear Instruments and Methods in Physics Research Section B: Beam Interactions with Materials and Atoms*, *258*(2), 403–413. https://doi.org/10.1016/j.nimb.2007.01.297

Okin, G. S., & Painter, T. H. (2004). Effect of grain size on remotely sensed spectral reflectance of sandy desert surfaces. *Remote Sensing of Environment*, *89*(3), 272–280. https://doi.org/10.1016/j.rse.2003.10.008

Opp, C., Groll, M., Abbasi, H., & Foroushani, M. A. (2021). Causes and effects of sand and dust storms: What has past research taught us? A survey. *Journal of Risk and Financial Management*, *14*(7), 326. https://doi.org/10.3390/jrfm14070326

Owen, P. R. (1964). Saltation of uniform grains in air. *Journal of Fluid Mechanics*, *20*, 225–242. https://doi.org/10.1017/s0022112064001173

Owen, J. J., Amundson, R., Dietrich, W. E., Nishiizumi, K., Sutter, B., & Chong, G. (2011). The sensitivity of hillslope bedrock erosion to precipitation. *Earth Surface Processes and Landforms*, *36*(1), 117–135. https://doi.org/10.1002/esp.2083

Pastore, G., Baird, T., Vermeesch, P., Resentini, A., & Garzanti, E. (2021). Provenance and recycling of Sahara Desert sand. *Earth-Science Reviews*, 103606. https://doi.org/10.1016/j.earscirev.2021.103606

Pearce, K. I., & Walker, I. J. (2005). Frequency and magnitude biases in the 'Fryberger'model, with implications for characterizing geomorphically effective winds. *Geomorphology*, *68*(1–2), 39–55. https://doi.org/10.1016/j.geomorph.2004.09.030

Prigent, C., Jiménez, C., & Catherinot, J. (2012). Comparison of satellite microwave backscattering (ASCAT) and visible/near-infrared reflectances (PARASOL) for the estimation of aeolian aerodynamic roughness length in arid and semi-arid regions. *Atmospheric Measurement Techniques*, *5*(11), 2703–2712. https://doi.org/10.5194/amt-5-2703-2012

Prigent, C., Tegen, I., Aires, F., Marticorena, B., & Zribi, M. (2005). Estimation of the aerodynamic roughness length in arid and semi-arid regions over the globe with the ERS scatterometer. *Journal of Geophysical Research: Atmospheres*, *110*(D9). https://doi.org/10.1029/2004jd005370

Raispour, K., Khosravi, M., Tavousi, T., & Sharifikiya, M. (2016). The influence of the polar front jet stream on the formation of dust events in the southwest of Iran. *Air Quality, Atmosphere & Health*, *9*(1), 15–23. https://doi.org/10.1007/s11869-014-0270-y

Rashki, A., Middleton, N., & Goudie, A. (2021). Dust storms in Iran—Distribution, causes, frequencies and impacts. *Aeolian Research*, *48*, 100655. https://doi.org/10.1016/j.aeolia.2020.100655

Reyre, D., & Mohafez, S. (1972). *A first contribution of the NIOC-ERAP agreements to the knowledge of Iranian geology*. Editions Technip Paris.

Rosen, M. R. (1994). The importance of groundwater in playas: A review of playa classifications and. *Geological Society of America Special Papers*, *289*, 1–18. https://doi.org/10.1130/spe289-p1

Rozier, O., Narteau, C., Gadal, C., Claudin, P., & Courrech du Pont, S. (2019). Elongation and stability of a linear dune. *Geophysical Research Letters*, *46*(24), 14521–14530. https://doi.org/10.1029/2019gl085147

Rubin, D., & Hunter, R. (1987). Bedform alignment in directionally varying flows. *Science*, *237*, 276–278. https://doi.org/10.1126/science.237.4812.276

Sabouri, J. (2008). *UNESCO World Heritage List – Lut Desert Gallery: Gandom Beryan*. Retrieved from https://whc.unesco.org/en/list/1505/gallery/

Sadler, P. M., & Jerolmack, D. J. (2015). Scaling laws for aggradation, denudation and progradation rates: The case for time-scale invariance at sediment sources and sinks. *Geological Society, London, Special Publications*, *404*(1), 69–88. https://doi.org/10.1144/sp404.7

Salles, T., Ding, X., Webster, J. M., Vila-Concejo, A., Brocard, G., & Pall, J. (2018). A unified framework for modelling sediment fate from source to sink and its interactions with reef systems over geological times. *Scientific Reports*, *8*(1), 1–11. https://doi.org/10.1038/s41598-018-23519-8

Sebe, K., Csillag, G., Ruszkiczay-Rüdiger, Z., Fodor, L., Thamó-Bozsó, E., Müller, P., et al. (2011). Wind erosion under cold climate: A Pleistocene periglacial mega-yardang system in Central Europe (Western Pannonian Basin, Hungary). *Geomorphology*, *134*(3–4), 470–482. https://doi.org/10.1016/j.geomorph.2011.08.003

Shao, Y., Wyrwoll, K.-H., Chappell, A., Huang, J., Lin, Z., McTainsh, G. H., et al. (2011). Dust cycle: An emerging core theme in Earth system science. *Aeolian Research*, *2*(4), 181–204. https://doi.org/10.1016/j.aeolia.2011.02.001

Sherman, D. J., & Farrell, E. J. (2008). Aerodynamic roughness lengths over movable beds: Comparison of wind tunnel and field data. *Journal of Geophysical Research: Earth Surface*, *113*(F02S08). https://doi.org/10.1029/2007jf000784

Shortridge, A., & Messina, J. (2011). Spatial structure and landscape associations of SRTM error. *Remote Sensing of Environment*, *115*(6), 1576–1587. https://doi.org/10.1016/j.rse.2011.02.017

Sømme, T. O., Helland-Hansen, W., Martinsen, O. J., & Thurmond, J. B. (2009). Relationships between morphological and sedimentological parameters in source-to-sink systems: A basis for predicting semi-quantitative characteristics in subsurface systems. *Basin Research*, *21*(4), 361–387.

Stilla, D., Zribi, M., Pierdicca, N., Baghdadi, N., & Huc, M. (2020). Desert roughness retrieval using CYGNSS GNSS-R data. *Remote Sensing*, *12*(4), 743. https://doi.org/10.3390/rs12040743

Stone, J. O. (2000). Air pressure and cosmogenic isotope production. *Journal of Geophysical Research: Solid Earth*, *105*(B10), 23753–23759. https://doi.org/10.1029/2000jb900181

Stull, R. B. (1988). *An introduction to boundary layer meteorology*. Kluwer Academic Publishers.

Sun, J. (2002). Provenance of loess material and formation of loess deposits on the Chinese Loess Plateau. *Earth and Planetary Science Letters*, *203*(3–4), 845–859. https://doi.org/10.1016/s0012-821x(02)00921-4

Thomas, D. S. (2011). *Arid zone geomorphology: Process, form and change in drylands*. John Wiley & Sons.

Tsoar, H. (2005). Sand dunes mobility and stability in relation to climate. *Physica A: Statistical Mechanics and its Applications*, *357*(1), 50–56. https://doi.org/10.1016/j.physa.2005.05.067

Ungar, J. E., & Haff, P. (1987). Steady state saltation in air. *Sedimentology*, *34*(2), 289–299. https://doi.org/10.1111/j.1365-3091.1987.tb00778.x

Van der Wateren, F. M., & Dunai, T. J. (2001). Late Neogene passive margin denudation history—Cosmogenic isotope measurements from the central Namib desert. *Global and Planetary Change*, *30*(3–4), 271–307. https://doi.org/10.1016/s0921-8181(01)00104-7

Von Blanckenburg, F. (2005). The control mechanisms of erosion and weathering at basin scale from cosmogenic nuclides in river sediment. *Earth and Planetary Science Letters*, *237*(3–4), 462–479. https://doi.org/10.1016/j.epsl.2005.06.030

Wagner, F., Bortoli, D., Pereira, S., Costa, M. J., Maria Silva, A., Weinzierl, B., et al. (2009). Properties of dust aerosol particles transported to Portugal from the Sahara desert. *Tellus B: Chemical and Physical Meteorology*, *61*(1), 297–306. https://doi.org/10.1111/j.1600-0889.2008.00393.x

Walker, R., Gans, P., Allen, M., Jackson, J., Khatib, M., Marsh, N., et al. (2009). Late Cenozoic volcanism and rates of active faulting in eastern Iran. *Geophysical Journal International*, *177*(2), 783–805. https://doi.org/10.1111/j.1365-246x.2008.04024.x

Wang, X., Dong, Z., Zhang, J., Qu, J., & Zhao, A. (2003). Grain size characteristics of dune sands in the central Taklimakan Sand Sea. *Sedimentary Geology*, *161*(1–2), 1–14. https://doi.org/10.1016/s0037-0738(02)00380-9

Wasson, R., & Hyde, R. (1983). Factors determining desert dune types. *Nature*, *304*, 337–339. https://doi.org/10.1038/304337a0

Wilson, I. G. (1971). Desert sandflow basins and a model for the development of ergs. *The Geographical Journal*, *137*(2), 180–199. https://doi.org/10.2307/1796738

Wood, W. W., & Sanford, W. E. (1990). Ground-water control of evaporite deposition. *Economic Geology*, *85*(6), 1226–1235. https://doi.org/10.2113/gsecongeo.85.6.1226

Wood, W. W., & Sanford, W. E. (1995). Eolian transport, saline lake basins, and groundwater solutes. *Water Resources Research*, *31*(12), 3121–3129. https://doi.org/10.1029/95wr02572

Xiao, Y., Shao, J., Frape, S. K., Cui, Y., Dang, X., Wang, S., et al. (2018). Groundwater origin, flow regime and geochemical evolution in arid endorheic watersheds: A case study from the Qaidam Basin, northwestern China. *Hydrology and Earth System Sciences*, *22*(8), 4381–4400. https://doi.org/10.5194/hess-22-4381-2018

Yechieli, Y., & Wood, W. W. (2002). Hydrogeologic processes in saline systems: Playas, sabkhas, and saline lakes. *Earth-Science Reviews*, *58*(3–4), 343–365. https://doi.org/10.1016/s0012-8252(02)00067-3

Zender, C. S., Miller, R., & Tegen, I. (2004). Quantifying mineral dust mass budgets: Terminology, constraints, and current estimates. *Eos, Transactions American Geophysical Union*, *85*(48), 509–512. https://doi.org/10.1029/2004eo480002

Zerathe, S., Blard, P.-H., Braucher, R., Bourles, D., Audin, L., Carcaillet, J., et al. (2017). Toward the feldspar alternative for cosmogenic ^{10}Be applications. *Quaternary Geochronology*, *41*, 83–96. https://doi.org/10.1016/j.quageo.2017.06.004

Zhang, D., Narteau, C., & Rozier, O. (2010). Morphodynamics of barchan and transverse dunes using a cellular automaton model. *Journal of Geophysical Research: Earth Surface*, *115*(F03041). https://doi.org/10.1029/2009JF001620

Zhang, D., Narteau, C., Rozier, O., & Courrech du Pont, S. (2012). Morphology and dynamics of star dunes from numerical modelling. *Nature Geoscience*, *5*, 463–467. https://doi.org/10.1038/ngeo1503

Zhang, C., Shen, Y., Li, Q., Jia, W., Li, J., & Wang, X. (2018). Sediment grain–size characteristics and relevant correlations to the aeolian environment in China's eastern desert region. *The Science of the Total Environment*, *627*, 586–599. https://doi.org/10.1016/j.scitotenv.2018.01.270

Reference From the Supporting Information

Aguilar, G., Carretier, S., Regard, V., Vassallo, R., Riquelme, R., & Martinod, J. (2014). Grain size-dependent ^{10}Be concentrations in alluvial stream sediment of the Huasco Valley, a semi-arid Andes region. *Quaternary Geochronology*, *19*, 163–172. https://doi.org/10.1016/j.quageo.2013.01.011

Al-Dousari, A., Al-Enezi, A., & Al-Awadhi, J. (2008). Textural variations within different representative types of dune sediments in Kuwait. *Arabian Journal of Geosciences*, *1*(1), 17–31. https://doi.org/10.1007/s12517-008-0002-4

Alizadeh-Choobari, O., Zawar-Reza, P., & Sturman, A. (2014b). The "wind of 120 days" and dust storm activity over the Sistan Basin. *Atmospheric Research*, *143*, 328–341. https://doi.org/10.1016/j.atmosres.2014.02.001

Bagnold, R. A. (1941). *The physics of wind blown sand and desert dunes*. Methuen.

Borchers, B., Marrero, S., Balco, G., Caffee, M., Goehring, B., Lifton, N., et al. (2016). Geological calibration of spallation production rates in the CRONUS-Earth project. *Quaternary Geochronology*, *31*, 188–198. https://doi.org/10.1016/j.quageo.2015.01.009

Braucher, R., Guillou, V., Bourlès, D., Arnold, M., Aumaître, G., Keddadouche, K., Nottoli, E. (2015). Preparation of ASTER in-house 10Be/9Be standard solutions. *Nuclear Instruments and Methods in Physics Research Section B: Beam Interactions with Materials and Atoms*, *361*, 335–340. https://doi.org/10.1016/j.nimb.2015.06.012

Braucher, R., Matmon, A., Bourlès, D., Aumaître, G., & Keddadouche, K. (2019). Towards successful cleaning of chert samples for improved ^{10}Be and ^{26}Al measurements. *Nuclear Instruments and Methods in Physics Research Section B: Beam Interactions with Materials and Atoms*, *456*, 257–263.

Braucher, R., Merchel, S., Borgomano, J., & Bourlès, D. (2011). Production of cosmogenic radionuclides at great depth: A multi element approach. *Earth and Planetary Science Letters*, *309*(1–2), 1–9. https://doi.org/10.1016/j.epsl.2011.06.036

Britter, R., Hunt, J., & Richards, K. (1981). Air flow over a two-dimensional hill: Studies of velocity speed-up, roughness effects and turbulence. *Quarterly Journal of the Royal Meteorological Society*, *107*(451), 91–110. https://doi.org/10.1002/qj.49710745106

Carretier, S., Regard, V., Vassallo, R., Aguilar, G., Martinod, J., Riquelme, R., et al. (2013). Slope and climate variability control of erosion in the Andes of central Chile. *Geology*, *41*(2), 195–198. https://doi.org/10.1130/g33735.1

Carretier, S., Regard, V., Vassallo, R., Aguilar, G., Martinod, J., Riquelme, R., et al. (2015). Differences in ^{10}Be concentrations between river sand, gravel and pebbles along the western side of the central Andes. *Quaternary Geochronology*, *27*, 33–51. https://doi.org/10.1016/j.quageo.2014.12.002

Chmeleff, J., von Blanckenburg, F., Kossert, K., & Jakob, D. (2010). Determination of the 10Be half-life by multicollector ICP-MS and liquid scintillation counting. *Nuclear Instruments and Methods in Physics Research Section B: Beam Interactions with Materials and Atoms*, *268*(2), 192–199. https://doi.org/10.1016/j.nimb.2009.09.012

Clapp, E. M., Bierman, P. R., Schick, A. P., Lekach, J., Enzel, Y., & Caffee, M. (2000). Sediment yield exceeds sediment production in arid region drainage basins. *Geology*, *28*(11), 995–998. https://doi.org/10.1130/0091-7613(2000)028<0995:syespi>2.3.co;2

Cockburn, H. A., Seidl, M. A., & Summerfield, M. A. (1999). Quantifying denudation rates on inselbergs in the central Namib Desert using in situ–produced cosmogenic ^{10}Be and ^{26}Al. *Geology*, *27*(5), 399–402. https://doi.org/10.1130/0091-7613(1999)027<0399:qdroii>2.3.co;2

Conrad, G., Montigny, R., Thuizat, R., & Westphal, M. (1981). Tertiary and Quaternary geodynamics of southern Lut (Iran) as deduced from palaeomagnetic, isotopic and structural data. *Tectonophysics*, *75*(3–4), T11–T17. https://doi.org/10.1016/0040-1951(81)90272-9

Day, M., & Kocurek, G. (2016). Observations of an aeolian landscape: From surface to orbit in Gale Crater. *Icarus*, *280*, 37–71. https://doi.org/10.1016/j.icarus.2015.09.042

Dickinson, W. W., & Ward, J. D. (1994). Low depositional porosity in eolian sands and sandstones, Namib Desert. *Journal of Sedimentary Research*, *64*(2a), 226–232. https://doi.org/10.1306/d4267d66-2b26-11d7-8648000102c1865d

Dunai, T. J., López, G. A. G., & Juez-Larré, J. (2005). Oligocene–Miocene age of aridity in the Atacama Desert revealed by exposure dating of erosion-sensitive landforms. *Geology*, *33*(4), 321–324. https://doi.org/10.1130/g21184.1

Durán, O., Claudin, P., & Andreotti, B. (2011). On aeolian transport: Grain-scale interactions, dynamical mechanisms and scaling laws. *Aeolian Research*, *3*(3), 243–270. https://doi.org/10.1016/j.aeolia.2011.07.006

Elbelrhiti, H., Claudin, P., & Andreotti, B. (2005). Field evidence for surface-wave-induced instability of sand dunes. *Nature*, *437*, 720–723. https://doi.org/10.1038/nature04058

Elkhrachy, I. (2018). Vertical accuracy assessment for SRTM and ASTER Digital Elevation Models: A case study of Najran city, Saudi Arabia. *Ain Shams Engineering Journal*, *9*(4), 1807–1817. https://doi.org/10.1016/j.asej.2017.01.007

Ewing, R. C., & Kocurek, G. A. (2010). Aeolian dune interactions and dune-field pattern formation: White Sands Dune Field, New Mexico. *Sedimentology*, *57*(5), 1199–1219. https://doi.org/10.1111/j.1365-3091.2009.01143.x

Ewing, R. C., McDonald, G. D., & Hayes, A. G. (2015). Multi-spatial analysis of aeolian dune-field patterns. *Geomorphology*, *240*, 44–53. https://doi.org/10.1016/j.geomorph.2014.11.023

Farr, T. G., Rosen, P. A., Caro, E., Crippen, R., Duren, R., Hensley, S., et al. (2007). The shuttle radar topography mission. *Reviews of Geophysics*, *45*(2). https://doi.org/10.1029/2005rg000183

Fernandez-Cascales, L., Lucas, A., Rodriguez, S., Gao, X., Spiga, A., & Narteau, C. (2018). First quantification of relationship between dune orientation and sediment availability, Olympia Undae, Mars. *Earth and Planetary Science Letters*, *489*, 241–250. https://doi.org/10.1016/j.epsl.2018.03.001

Field, J., & Pelletier, J. (2018). Controls on the aerodynamic roughness length and the grain-size dependence of aeolian sediment transport. *Earth Surface Processes and Landforms*, *43*, 2616–2626. https://doi.org/10.1002/esp.4420

Gadal, C., Narteau, C., Courrech du Pont, S., Rozier, O., & Claudin, P. (2019). Incipient bedforms in a bidirectional wind regime. *Journal of Fluid Mechanics*, *862*, 490–516. https://doi.org/10.1017/jfm.2018.978

Gao, X., Narteau, C., & Rozier, O. (2015). Development and steady states of transverse dunes: A numerical analysis of dune pattern coarsening and giant dunes. *Journal of Geophysical Research: Earth Surface*, *120*, 2200–2219. https://doi.org/10.1002/2015JF003549

Harel, M.-A., Mudd, S., & Attal, M. (2016). Global analysis of the stream power law parameters based on worldwide ^{10}Be denudation rates. *Geomorphology*, *268*, 184–196. https://doi.org/10.1016/j.geomorph.2016.05.035

Iversen, J. D., Greeley, R., Marshall, J. R., & Pollack, J. B. (1987). Aeolian saltation threshold: The effect of density ratio. *Sedimentology*, *34*(4), 699–706. https://doi.org/10.1111/j.1365-3091.1987.tb00795.x

Jackson, P. S., & Hunt, J. C. R. (1975). Turbulent wind flow over a low hill. *Quarterly Journal of the Royal Meteorological Society*, *101*, 929–955. https://doi.org/10.1002/qj.49710143015

Jayko, A. (2005). Late Quaternary denudation, Death and Panamint valleys, eastern California. *Earth-Science Reviews*, *73*(1–4), 271–289. https://doi.org/10.1016/j.earscirev.2005.04.009

Johnson, K. S. (1997). Evaporite karst in the United States. *Carbonates and Evaporites*, *12*(1), 2–14. https://doi.org/10.1007/bf03175797

Jolivet, M., Braucher, R., Dovchintseren, D., Hocquet, S., Schmitt, J.-M., Team, A., et al. (2021). Erosion around a large-scale topographic high in a semi-arid sedimentary basin: Interactions between fluvial erosion, aeolian erosion and aeolian transport. *Geomorphology*, *386*, 107747. https://doi.org/10.1016/j.geomorph.2021.107747

Kapp, P., Pelletier, J. D., Rohrmann, A., Heermance, R., Russell, J., Ding, L., et al. (2011). Wind erosion in the Qaidam basin, central Asia: Implications for tectonics, paleoclimate, and the source of the Loess Plateau. *Geological Society of America Today*, *21*(4/5), 4–10. https://doi.org/10.1130/gsatg99a.1

Kober, F., Ivy-Ochs, S., Schlunegger, F., Baur, H., Kubik, P., & Wieler, R. (2007). Denudation rates and a topography-driven rainfall threshold in northern Chile: Multiple cosmogenic nuclide data and sediment yield budgets. *Geomorphology*, *83*(1–2), 97–120. https://doi.org/10.1016/j.geomorph.2006.06.029

Kober, F., Ivy-Ochs, S., Zeilinger, G., Schlunegger, F., Kubik, P. W., Baur, H., et al. (2009). Complex multiple cosmogenic nuclide concentration and histories in the arid Rio Lluta catchment, northern Chile. *Earth Surface Processes and Landforms*, *34*(3), 398–412. https://doi.org/10.1002/esp.1748

Korschinek, G., Bergmaier, A., Faestermann, T., Gerstmann, U., Knie, K., Rugel, G., et al. (2010). A new value for the half-life of 10Be by heavy-ion elastic recoil detection and liquid scintillation counting. *Nuclear Instruments and Methods in Physics Research Section B: Beam Interactions with Materials and Atoms*, *268*(2), 187–191. https://doi.org/10.1016/j.nimb.2009.09.020

Lal, D. (1991). Cosmic ray labeling of erosion surfaces: In situ nuclide production rates and erosion models. *Earth and Planetary Science Letters*, *104*(2–4), 424–439. https://doi.org/10.1016/0012-821x(91)90220-c

Laurent, B., Marticorena, B., Bergametti, G., Chazette, P., Maignan, F., & Schmechtig, C. (2005). Simulation of the mineral dust emission frequencies from desert areas of China and Mongolia using an aerodynamic roughness length map derived from the POLDER/ADEOS 1 surface products. *Journal of Geophysical Research: Atmospheres*, *110*(D18). https://doi.org/10.1029/2004jd005013

Livingstone, I. (1987). Grain-size variation on a 'complex' linear dune in the Namib Desert. *Geological Society, London, Special Publications*, *35*(1), 281–291. https://doi.org/10.1144/gsl.sp.1987.035.01.19

Lü, P., Narteau, C., Dong, Z., Claudin, P., Rodriguez, S., An, Z., et al. (2021). Direct validation of dune instability theory. *Proceedings of the National Academy of Sciences*, *118*(17). https://doi.org/10.1073/pnas.2024105118

Lü, P., Narteau, C., Dong, Z., Rozier, O., & Courrech Du Pont, S. (2017). Unravelling raked linear dunes to explain the coexistence of bedforms in complex dunefields. *Nature Communications*, *8*, 14239. https://doi.org/10.1038/ncomms14239

Marticorena, B., Chazette, P., Bergametti, G., Dulac, F., & Legrand, M. (2004). Mapping the aerodynamic roughness length of desert surfaces from the POLDER/ADEOS bi-directional reflectance product. *International Journal of Remote Sensing*, *25*(3), 603–626. https://doi.org/10.1080/0143116031000116976

Matmon, A., Simhai, O., Amit, R., Haviv, I., Porat, N., McDonald, E., et al. (2009). Desert pavement–coated surfaces in extreme deserts present the longest-lived landforms on Earth. *The Geological Society of America Bulletin*, *121*(5–6), 688–697. https://doi.org/10.1130/b26422.1

McPhillips, D., Bierman, P. R., Crocker, T., & Rood, D. H. (2013). Landscape response to Pleistocene-Holocene precipitation change in the Western Cordillera, Peru: 10Be concentrations in modern sediments and terrace fills. *Journal of Geophysical Research: Earth Surface*, *118*(4), 2488–2499. https://doi.org/10.1002/2013jf002837

Merchel, S., & Bremser, W. (2004). First international 26Al interlaboratory comparison—Part I. *Nuclear Instruments and Methods in Physics Research Section B: Beam Interactions with Materials and Atoms*, *223*, 393–400. https://doi.org/10.1016/j.nimb.2004.04.076

Morris, D. A., & Johnson, A. I. (1967). *Summary of hydrologic and physical properties of rock and soil materials, as analyzed by the hydrologic laboratory of the US Geological Survey, 1948-60* (Tech. Rep.). US Government Printing Office

Muñoz Sabater, J. (2019). *ERA5-Land hourly data from 1981 to present. Copernicus Climate Change Service (C3S) Climate Data Store (CDS)*.

Narteau, C., Zhang, D., Rozier, O., & Claudin, P. (2009). Setting the length and time scales of a cellular automaton dune model from the analysis of superimposed bed forms. *Journal of Geophysical Research: Earth Surface*, *114*, F03006. https://doi.org/10.1029/2008JF001127

Nishiizumi, K. (2004). Preparation of 26Al AMS standards. *Nuclear Instruments and Methods in Physics Research Section B: Beam Interactions with Materials and Atoms*, *223*, 388–392. https://doi.org/10.1016/j.nimb.2004.04.075

Nishiizumi, K., Imamura, M., Caffee, M. W., Southon, J. R., Finkel, R. C., & McAninch, J. (2007). Absolute calibration of 10Be AMS standards. *Nuclear Instruments and Methods in Physics Research Section B: Beam Interactions with Materials and Atoms*, *258*(2), 403–413. https://doi.org/10.1016/j.nimb.2007.01.297

Okin, G. S., & Painter, T. H. (2004). Effect of grain size on remotely sensed spectral reflectance of sandy desert surfaces. *Remote Sensing of Environment*, *89*(3), 272–280. https://doi.org/10.1016/j.rse.2003.10.008

Owen, P. R. (1964). Saltation of uniform grains in air. *Journal of Fluid Mechanics*, *20*, 225–242. https://doi.org/10.1017/s0022112064001173

Owen, J. J., Amundson, R., Dietrich, W. E., Nishiizumi, K., Sutter, B., & Chong, G. (2011). The sensitivity of hillslope bedrock erosion to precipitation. *Earth Surface Processes and Landforms*, *36*(1), 117–135. https://doi.org/10.1002/esp.2083

Prigent, C., Jiménez, C., & Catherinot, J. (2012). Comparison of satellite microwave backscattering (ASCAT) and visible/near-infrared reflectances (PARASOL) for the estimation of aeolian aerodynamic roughness length in arid and semi-arid regions. *Atmospheric MeasurementTechniques*, *5*(11), 2703–2712. https://doi.org/10.5194/amt-5-2703-2012

Prigent, C., Tegen, I., Aires, F., Marticorena, B., & Zribi, M. (2005). Estimation of the aerodynamic roughness length in arid and semi-arid regionsover the globe with the ERS scatterometer. *Journal of Geophysical Research: Atmospheres*, *110*(D9). https://doi.org/10.1029/2004jd005370

Raispour, K., Khosravi, M., Tavousi, T., & Sharifikiya, M. (2016). The influence of the polar front jet stream on the formation of dust events inthe southwest of Iran. *Air Quality, Atmosphere & Health*, *9*(1), 15–23. https://doi.org/10.1007/s11869-014-0270-y

Rosen, M. R. (1994). The importance of groundwater in playas: A review of playa classifications and. *Geological Society of America Special Papers*, *289*, 1–18. https://doi.org/10.1130/spe289-p1

Rubin, D., & Hunter, R. (1987). Bedform alignment in directionally varying flows. *Science*, *237*, 276–278. https://doi.org/10.1126/science.237.4812.276

Sabouri, J. (2008). *UNESCO World Heritage List – Lut Desert Gallery: Gandom Beryan*. Retrieved from https://whc.unesco.org/en/list/1505/gallery/

Sebe, K., Csillag, G., Ruszkiczay-Rüdiger, Z., Fodor, L., Thamó-Bozsó, E., Müller, P., et al. (2011). Wind erosion under cold climate: A Pleistocene periglacial mega-yardang system in Central Europe (Western Pannonian Basin, Hungary). *Geomorphology*, *134*(3–4), 470–482. https://doi.org/10.1016/j.geomorph.2011.08.003

Sherman, D. J., & Farrell, E. J. (2008). Aerodynamic roughness lengths over movable beds: Comparison of wind tunnel and field data. *Journalof Geophysical Research: Earth Surface*, *113*(F02S08). https://doi.org/10.1029/2007jf000784

Shortridge, A., & Messina, J. (2011). Spatial structure and landscape associations of SRTM error. *Remote Sensing of Environment*, *115*(6),1576–1587. https://doi.org/10.1016/j.rse.2011.02.017

Starke, J., Ehlers, T., & Schaller, M. (2017). Tectonic and climatic controls on the spatial distribution of denudation rates in Northern Chile (18 S to 23 S) determined from cosmogenic nuclides. *Journal of Geophysical Research: Earth Surface*, *122*(10), 1949–1971. https://doi.org/10.1002/2016jf004153

Stilla, D., Zribi, M., Pierdicca, N., Baghdadi, N., & Huc, M. (2020). Desert roughness retrieval using CYGNSS GNSS-R data. *Remote Sensing*,*12*(4), 743. https://doi.org/10.3390/rs12040743

Stone, J. O. (2000). Air pressure and cosmogenic isotope production. *Journal of Geophysical Research: Solid Earth*, *105*(B10), 23753–23759. https://doi.org/10.1029/2000jb900181

Stull, R. B. (1988). *An introduction to boundary layer meteorology*. Kluwer Academic Publishers

Van der Wateren, F. M., & Dunai, T. J. (2001). Late Neogene passive margin denudation history—Cosmogenic isotope measurements from thecentral Namib desert. *Global and Planetary Change*, *30*(3–4), 271–307. https://doi.org/10.1016/s0921-8181(01)00104-7

Von Blanckenburg, F. (2005). The control mechanisms of erosion and weathering at basin scale from cosmogenic nuclides in river sediment.*Earth and Planetary Science Letters*, *237*(3–4), 462–479. https://doi.org/10.1016/j.epsl.2005.06.030

Wagner, F., Bortoli, D., Pereira, S., Costa, M. J., Maria Silva, A., Weinzierl, B., et al. (2009). Properties of dust aerosol particles transported to Portugal from the Sahara desert. *Tellus B: Chemical and Physical Meteorology*, *61*(1), 297–306. https://doi.org/10.1111/j.1600-0889.2008.00393.x

Wang, X., Dong, Z., Zhang, J., Qu, J., & Zhao, A. (2003). Grain size characteristics of dune sands in the central Taklimakan Sand Sea. *Sedimentary Geology*, *161*(1–2), 1–14. https://doi.org/10.1016/s0037-0738(02)00380-9

Wood, W. W., & Sanford, W. E. (1990). Ground-water control of evaporite deposition. *Economic Geology*, *85*(6), 1226–1235. https://doi.org/10.2113/gsecongeo.85.6.1226

Wood, W. W., & Sanford, W. E. (1995). Eolian transport, saline lake basins, and groundwater solutes. *Water Resources Research*, *31*(12),3121–3129. https://doi.org/10.1029/95wr02572

Xiao, Y., Shao, J., Frape, S. K., Cui, Y., Dang, X., Wang, S., et al. (2018). Groundwater origin, flow regime and geochemical evolution in ariendorheic watersheds: A case study from the Qaidam Basin, northwestern China. *Hydrology and Earth System Sciences*, *22*(8), 4381–4400. https://doi.org/10.5194/hess-22-4381-2018

Yechieli, Y., & Wood, W. W. (2002). Hydrogeologic processes in saline systems: Playas, sabkhas, and saline lakes. *Earth-Science Reviews*,*58*(3–4), 343–365. https://doi.org/10.1016/s0012-8252(02)00067-3

Zerathe, S., Blard, P.-H., Braucher, R., Bourles, D., Audin, L., Carcaillet, J., et al. (2017). Toward the feldspar alternative for cosmogenic 10Beapplications. *Quaternary Geochronology*, *41*, 83–96. https://doi.org/10.1016/j.quageo.2017.06.004

Zhang, D., Narteau, C., & Rozier, O. (2010). Morphodynamics of barchan and transverse dunes using a cellular automaton model. *Journal ofGeophysical Research: Earth Surface*, *115*(F03041). https://doi.org/10.1029/2009JF001620

Zhang, D., Narteau, C., Rozier, O., & Courrech du Pont, S. (2012). Morphology and dynamics of star dunes from numerical modelling. *NatureGeoscience*, *5*, 463–467. https://doi.org/10.1038/ngeo1503

Zhang, C., Shen, Y., Li, Q., Jia, W., Li, J., & Wang, X. (2018). Sediment grain–size characteristics and relevant correlations to the aeolian environment in China's eastern desert region. *The Science of the Total Environment*, *627*, 586–599. https://doi.org/10.1016/j.scitotenv.2018.01.270